

See discussions, stats, and author profiles for this publication at: <https://www.researchgate.net/publication/223987744>

Cardiac Myosin Binding Protein C and Its Phosphorylation Regulate Multiple Steps in the Cross-Bridge Cycle of Muscle Contraction

ARTICLE *in* BIOCHEMISTRY · APRIL 2012

Impact Factor: 3.02 · DOI: 10.1021/bi300085x · Source: PubMed

CITATIONS

14

READS

22

2 AUTHORS:



[Arthur T Coulton](#)

Case Western Reserve University

11 PUBLICATIONS 192 CITATIONS

SEE PROFILE



[Julian E Stelzer](#)

Case Western Reserve University

42 PUBLICATIONS 967 CITATIONS

SEE PROFILE

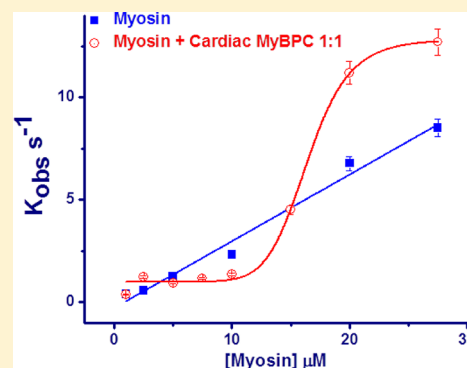
Cardiac Myosin Binding Protein C and Its Phosphorylation Regulate Multiple Steps in the Cross-Bridge Cycle of Muscle Contraction

Arthur T. Coulton and Julian E. Stelzer*

Department of Physiology and Biophysics, School of Medicine, Case Western Reserve University, Cleveland, Ohio 44106, United States

Supporting Information

ABSTRACT: Cardiac myosin binding protein C (c-MyBPC) is a thick filament protein that is expressed in cardiac sarcomeres and is known to interact with myosin and actin. While both structural and regulatory roles have been proposed for c-MyBPC, its true function is unclear; however, phosphorylation has been shown to be important. In this study, we investigate the effect of c-MyBPC and its phosphorylation on two key steps of the cross-bridge cycle using fast reaction kinetics. We show that unphosphorylated c-MyBPC complexed with myosin in 1:1 and 3:1 myosin:c-MyBPC stoichiometries regulates the binding of myosin to actin (K_D) cooperatively (Hill coefficient, h) ($K_D = 16.44 \pm 0.33 \mu\text{M}$, and $h = 9.24 \pm 1.34$; $K_D = 11.48 \pm 0.75 \mu\text{M}$, and $h = 3.54 \pm 0.67$) and significantly decelerates the ATP-induced dissociation of myosin from actin (K_1k_{+2} values of 0.12 ± 0.01 and $0.22 \pm 0.01 \text{ M}^{-1} \text{ s}^{-1}$, respectively, compared with a value of $0.42 \pm 0.01 \text{ M}^{-1} \text{ s}^{-1}$ for myosin alone). Phosphorylation of c-MyBPC abolished the regulation of the association phase (K_1k_{+2} values of 0.32 ± 0.02 and $0.33 \pm 0.01 \text{ M}^{-1} \text{ s}^{-1}$ at 1:1 and 3:1 myosin:c-MyBPC ratios, respectively) and also accelerated the dissociation of myosin from actin (K_1k_{+2} values of 0.23 ± 0.01 and $0.29 \pm 0.01 \text{ M}^{-1} \text{ s}^{-1}$ at a 1:1 and 3:1 myosin:c-MyBPC ratios, respectively) relative to the dissociation of myosin from actin in the presence of unphosphorylated c-MyBPC. These results indicate a direct effect of c-MyBPC on cross-bridge kinetics that is independent of the thin filament that together with its phosphorylation provides a mechanism for fine-tuning cross-bridge behavior to match the contractile requirements of the heart.



Cardiac myosin binding protein C (c-MyBPC) is a thick filament-associated, sarcomeric protein located in discrete transverse bands in the C zone of the A band, which consists of eight immunoglobulin-like domains and three fibronectin type 3 domains that are designated C0–C10. These domains have been shown to specifically bind to the myosin tail (C10),¹ titin (C8–C10),² myosin subfragment 2 (S2) (C1–C2), and actin (C0–C1).^{3,4} The cardiac isoform includes a cardiac specific domain motif or m domain between C1 and C2 that undergoes phosphorylation by cAMP-dependent protein kinase A (PKA) in response to β -adrenergic agonists⁵ to affect cardiac output, and a proline/alanine rich linker connecting C0 and C1 that has been proposed to contain a possible actin binding region.⁴

c-MyBPC is being increasingly shown to have an important role in the regulation of muscle contraction; however, the precise mechanism is still unclear. Most data show the effects of c-MyBPC regulation in the presence of the thin filament. Some reports suggest that there is a direct interaction with tropomyosin (Tm),⁶ and others suggest that c-MyBPC is important for regulating force generation in fibers;^{7,8} however, whether the regulatory effects of c-MyBPC are due to a change in the inherent properties of cross-bridge formation and whether c-MyBPC acts in a manner that is independent of the thin filament regulatory proteins are unknown. Mutations in c-MyBPC are a leading cause of familial hypertrophic cardiomyopathy (FHC), which further underlines its necessity

for normal cardiac function.⁹ c-MyBPC knockout (KO) mice display an overall sarcomere structure that is unaffected but exhibit symptoms of cardiac hypertrophy,¹⁰ suggesting that c-MyBPC is not required for sarcomere assembly but for correct sarcomere function. This is further reinforced by studies with c-MyBPC KO mice that show that the lack of c-MyBPC accelerates cross-bridge cycling and rates of force development and increases shortening velocity and rates of force redevelopment and relaxation in permeabilized muscle fibers.^{7,11–13}

As a potential mechanism to account for the effects of c-MyBPC in limiting myofilament contractile properties, Hoffman and colleagues proposed a model in which c-MyBPC acts as an internal load within the thick filament that opposes shortening in such a way that c-MyBPC is tethered to myosin S2, thereby limiting myosin head position and/or mobility,¹⁴ and this idea was further examined in the work of Calaghan and colleagues.¹⁵ The tethering model may have an important part to play in c-MyBPC's regulation of contractile function; however, it is unclear that it accounts for the entire mechanism. Studies containing only the C1–C2 fragment with the associated phosphorylation sites of c-MyBPC showed that

Received: January 19, 2012

Revised: March 28, 2012

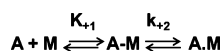
Published: March 29, 2012



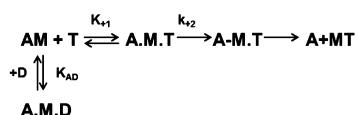
this fragment can affect contractile function alone in myocytes, and the ability of heavy meromyosin to move actin in *in vitro* motility assays without the remaining c-MyBPC domains and most significantly without the light meromyosin (LMM) binding domains, which is central to the idea of a tethering mechanism.^{16–18} Other studies have shown that the C0–C1 N-terminal region of c-MyBPC can bind the S1–S2 hinge region of myosin in a manner that is independent of a tether mechanism; however, although necessary, the regulatory role of the C0–C1 domain of c-MyBPC is unclear.¹⁹ Several investigations using *in vitro* biochemistry methods^{17–21} and structural methods^{6,22–27} have also provided evidence that the C0–C1 and C1–C2 regions of c-MyBPC may bind F actin in addition to binding the S2 region of myosin, and a further structural study has suggested that most of the N-terminal domains bind and are ordered on actin in such a way that they can modulate Tm function as well as block binding of myosin to actin.⁶ PKA-mediated phosphorylation of c-MyBPC is believed to accelerate cross-bridge kinetics,^{5,16,28} as many studies involving skinned fibers have shown increases in rates of force development and stretch activation in response to PKA stimulation;^{28–31} however, other studies do not support this view.^{32,33} The exact mechanism therefore is still unknown, and it has not been demonstrated whether c-MyBPC affects discrete steps of the cross-bridge cycle. Fiber and *in vitro* motility studies do not record discrete measurements of individual steps in the cross-bridge cycle of muscle contraction. It is therefore very difficult to apportion observations seen in the experiments when c-MyBPC is present to specific kinetic interactions. The stopped-flow assay has a long track record in measuring cross-bridge kinetics. It is able to accurately measure the fast reaction rates, but more importantly, it allows the measurement of kinetics of specific steps during muscle contraction. It is therefore possible to measure the effects of c-MyBPC and its phosphorylation at each stage of the cross-bridge cycle of muscle contraction.

The binding of S1 to actin and the hydrolysis of ATP with the subsequent dissociation of the two binding partners are two of the principal steps in the cross-bridge cycle of muscle contraction and can be described by Schemes 1 and 2. Both

Scheme 1. Myosin Binding to Actin



Scheme 2. ATP-Induced Dissociation of Myosin from Actin



steps are very rapid events; e.g., in the absence of ATP, myosin binds actin in solution with a very high affinity ($K_{\text{ass}} \approx 10^7 \text{ M}^{-1}$) to form the actomyosin complex, but the presence of ATP reduces the association constant to $<10^4 \text{ M}^{-1}$. The cross-bridge cycle has been extensively studied, but only in the absence of thick filament regulatory proteins, and defining the regulation of c-MyBPC on specific steps in the cross-bridge cycle is a prerequisite for improving our understanding of muscle contraction. This is very important as c-MyBPC is indicated in almost 40% of all hypertrophic cardiomyopathies (HCM);⁹ therefore, improving our understanding of how c-MyBPC

works will give us a better understanding of the pathophysiology of this disease. This is important for devising sarcomere treatment-based therapies for the treatment of HCM and heart failure such as that featured in the study of Malik.³⁴ The purpose of this study, therefore, is to define how c-MyBPC directly affects the kinetics of key steps in the cross-bridge cycle. The mechanism of c-MyBPC regulation as described above is still unclear, and there is currently no information regarding its effects on the kinetics of the key steps in the cross-bridge cycle of muscle contraction or whether cross-bridge regulation occurs in a manner that is independent of the thin filament regulatory proteins. It is possible that like another thick filament protein, regulatory light chain (RLC), which has been shown to modulate cross-bridge cycling in skeletal muscle³⁵ and cardiac muscle³⁶ in a phosphorylation-dependent manner, c-MyBPC may be a critical thick filament regulator of muscle contraction.

The current widely accepted model for the cross-bridge cycle of muscle contraction was presented by Geeves et al. in 1984.³⁷ This model consists of an ATPase-driven cycle of cross-bridge attachment, cross-bridge “rotation”, and ligand dissociation and binding where strain is an important factor.³⁸ The binding of myosin to actin and thus the cross-bridge cycle are regulated by thin filament proteins in a Ca^{2+} -dependent manner in both skeletal and cardiac muscle,^{39,40} whereby Tm sterically blocks the myosin binding sites on actin in the absence of Ca^{2+} .^{41,42}

In this study, we have prepared full-length c-MyBPC purified from porcine ventricular tissue because this system closely resembles the human heart in terms of the expression profile of contractile proteins as well as *in vivo* function. Stopped-flow measurements using full-length myosin and actin were conducted in the absence and presence of c-MyBPC, and the ATPase activity of the myosin motor was also investigated using the NADH-coupled system. In this way, we were able to quantify the effects of c-MyBPC and its phosphorylation on both transient and steady-state kinetics of critical steps in the cross-bridge cycle that govern the regulation of cardiac muscle contraction.

■ EXPERIMENTAL PROCEDURES

Preparation of Contractile Proteins. c-MyBPC protein was purified from porcine left ventricular tissue using the method of Hartzell and Windfield.⁴³ Briefly, 150 g of porcine left ventricular tissue was homogenized in 750 mL of buffer A [50 mM KCl, 2 mM EDTA, 20 mM Tris-HCl (pH 7.9), and 15 mM 2-mercaptoethanol] for approximately 2 min in a Waring blender. The homogenate was centrifuged at 3000g for 15 min. The pellet was washed three times with buffer A, twice more with buffer A containing 1% Triton, and a further three times with buffer A. The final pellets were resuspended with a polytron homogenizer in 400 mL of EDTA- PO_4 buffer (pH 5.9) (10 mM EDTA- Na_2 , 124 mM Na_2HPO_4 , and 31 mM Na_2HPO_4). The homogenate was centrifuged at 10000g for 20 min, and the resulting pellet was extracted a second time. The two supernatants were pooled and concentrated by ammonium sulfate precipitation (55% saturation). The precipitated protein was dissolved in 300 mM NaCl, 5.2 mM K_2HPO_4 , 4.8 mM Na_2HPO_4 , 2 mM NaN_3 , 0.1 mM EDTA, and 3 mM 2-mercaptoethanol and dialyzed overnight. The protein extract was then chromatographed according to the method of Starr and Offer.⁴⁴ The purity of the c-MyBPC protein was assessed by sodium dodecyl sulfate–polyacrylamide gel electrophoresis (SDS–PAGE). Cardiac myosin from porcine left ventricular

tissue was prepared according to the method of Taylor and Weeds,⁴⁵ and porcine skeletal actin was prepared according to the method of Spudich and Watt.⁴⁶

PKA Phosphorylation of c-MyBPC. The exogenous catalytic subunit of PKA from bovine heart (Sigma) was used to phosphorylate c-MyBPC according to the method of Tong et al.²⁹ The PKA catalytic subunit was resuspended in a 60 mM KCl, 10 mM MgCl₂, 2 mM ATP buffer such that the concentration was 100 units/ μ L, and this was added to the c-MyBPC protein solution to give a final PKA concentration of 1 unit/ μ L, where 1 unit is defined as the quantity of enzyme that will transfer 1.0 pmol of phosphate from [γ -³²P]ATP to hydrolyzed and partially dephosphorylated casein per minute at pH 6.5 and 30 °C. The c-MyBPC/PKA solution was incubated at 30 °C for 1 h, and the resulting sample was checked for the presence of phosphorylated c-MyBPC by Pro-Q Diamond staining (Molecular Probes) according to the manufacturer's protocol.

Immunological Techniques. The phosphorylation states of the three known c-MyBPC residues that are targets for PKA phosphorylation (i.e., serines 275, 284, and 304, of the human c-MyBPC sequence) were probed using phospho-specific antibodies raised against phosphate-conjugated serine 275, 284, and 304 peptides in SPF rabbits (21st Century Biochemicals, Marlboro, MA) and were subsequently affinity purified. Western blots were used to determine the relative level of basal and PKA-induced phosphorylation of residues 275, 284, and 304. To allow the rabbit purified anti-serine 275, 284, and 304 were used at a dilution of 1:500, and an anti-rabbit horseradish peroxidase secondary antibody was used at a dilution of 1:5000 for detection and qualitative comparison. Total c-MyBPC levels were also probed with a c-MyBPC specific antibody (Santa Cruz) at a dilution of 1:500. Blots were scanned and quantified using a FluorChem E imaging system (proteinsimple, Santa Clara, CA).

Transient Kinetic Measurements. All rapid kinetic measurements were performed with a standard Applied Photophysics stopped-flow system. Pyrene fluorescence was excited at 365 nm and monitored through a KV389 filter. The reactant concentrations stated in the text and figures are those after mixing in the stopped flow, unless stated otherwise. All experiments were conducted at 25 °C in buffer containing 20 mM MOPS (pH 7.0), 500 mM KCl, and 5 mM MgCl₂.

ATPase Assays. The steady-state ATPase activity of myosin in the absence and presence of c-MyBPC was measured using the NADH-coupled assay^{47,48} in a TECAN Infinite M1000 pro fluorescent plate reader. Increasing concentrations of myosin and c-MyBPC were mixed with 3.5 μ M actin in a solution of 20 mM MOPS (pH 7.0), 500 mM KCl, and 10 mM MgCl₂. The reaction was started by mixing the protein solution with an equal volume of 2 \times reaction mix (2 mM phosphoenolpyruvate, 1.2 μ M NADH, 10 mM ATP, and 0.04 unit/ μ L pyruvate kinase/lactate dehydrogenase), and the absorbance of NADH at 340 nm was monitored. Readings were taken every minute for 1 h or until the reaction went to completion. The absorbance at 340 nm was converted to ADP concentration and plotted versus time. ATPase rates were calculated from the slope of the graph and plotted as a function of myosin concentration.

All stopped-flow and ATPase assays were conducted with myosin and c-MyBPC present at a 1:1 ratio or at physiological myosin:c-MyBPC ratios of 3:1 or 7:1 as described by Craig et al.⁴⁹

Statistical Analysis. Steady-state and transient cross-bridge kinetics in the absence and presence of c-MyBPC were compared by one-way analysis of variance (ANOVA) or a Student's *t* test as appropriate. Measurements performed prior to and following c-MyBPC phosphorylation were compared by a Student's *t* test. Data were averaged from at least three separate experiments, and *P* values of <0.05 were considered statistically significant.

RESULTS

Protein Preparation. c-MyBPC was extracted and purified from porcine hearts to produce ~50 mg of protein from ~150 g of starting tissue. The purified protein seen in Figure 1A

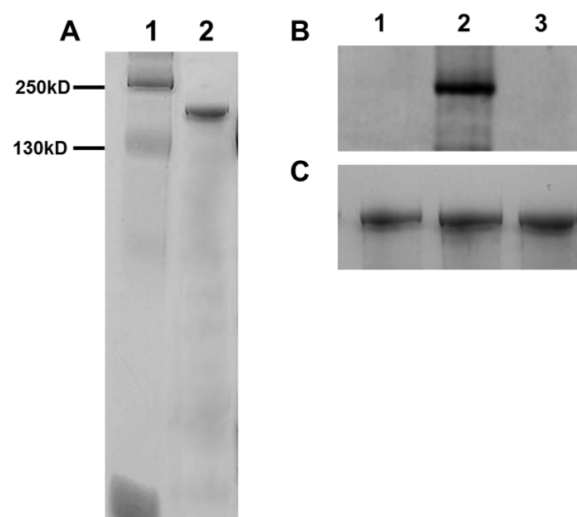


Figure 1. Gel electrophoresis and phosphorylation analysis of purified porcine c-MyBPC. (A) SDS-PAGE (12.5%) Coomassie Blue-stained gel showing the purity of full-length purified porcine c-MyBPC used in this study. The molecular masses of the markers are reported in lane 1. Lane 2 contained purified c-MyBPC, which is represented as an ~140 kDa band on the SDS-PAGE gel. (B) Pro-Q Diamond staining of untreated c-MyBPC (control lane 1) and c-MyBPC treated with PKA (lane 2) or calf intestinal alkaline phosphatase (lane 3). (C) Corresponding Coomassie Blue staining demonstrating equivalent protein loads for the three groups.

produced a single band on a 10% SDS-PAGE gel of ~140 kDa, which corresponded to values from previously published studies involving endogenous c-MyBPC. Figure 1B shows the effects of PKA treatment on purified endogenous c-MyBPC. Purified endogenous c-MyBPC was virtually unphosphorylated, like a protein treated with alkaline phosphatase; however, treatment with PKA using the method of Tong et al.²⁹ produced a robust band concomitant with the c-MyBPC protein. To determine the relative levels of PKA-induced phosphorylation at individual c-MyBPC phosphorylation residues prior to and following PKA treatment, phospho-specific antibodies for serines 275, 284, and 304 were used and Western blot analysis was conducted (Figure 1S of the Supporting Information). Similar to results from Pro-Q Diamond phosphorylation staining, basal phosphorylation levels prior to PKA treatment were low in residues 275 and 284 and not detected in residue 304; however, PKA treatment produced a significant increase in the magnitude of the phosphorylation signal in all three residues. Further analysis of the PKA signal size was conducted by quantifying the relative

signal obtained at residues 275, 284, and 304 prior to and following PKA treatment. The analysis showed that the magnitude of the signal produced by the phosphorylation of c-MyBPC was ~4- and ~5-fold higher at residues 275 and 284, respectively, than the magnitude of the unphosphorylated signal. The relative change in the phosphorylation signal due to PKA treatment at residue 304 could not be accurately determined because of the absence of a basal phosphorylation signal. It is important to note that although our data confirm that PKA does phosphorylate all three residues, our analysis does not provide direct information about the actual stoichiometry of the phosphorylation at each residue.

Myosin_c-MyBPC Binding to Actin. The binding of the myosin_c-MyBPC complex to actin can be followed by monitoring the decrease in fluorescence of pyrene-labeled actin (pyr.actin). Figure 2A shows representative fluorescence

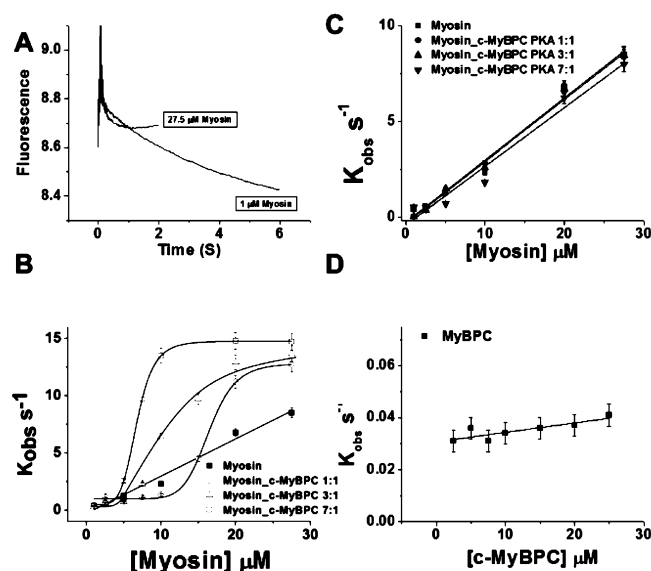


Figure 2. Binding of the myosin_c-MyBPC complex to actin. (A) Representative transients for the binding of low (1 μM) and excess concentrations of myosin_c-MyBPC (27.5 μM) to 1 μM pyrene-labeled actin at 25 $^{\circ}\text{C}$. The observed rate constant K_{obs} was calculated by fitting the transients to a single-exponential equation. Conditions: 20 mM MOPS (pH 7.0), 500 mM KCl, and 5 mM MgCl_2 . (B) K_{obs} plotted as a function of myosin concentration for myosin (■) and 7:1 (□), 3:1 (Δ), and 1:1 (○) myosin_c-MyBPC complexes. The second-order rate constants (K_1k_{+2}) in the absence of c-MyBPC were determined by a linear fit of the data. The equilibrium constant K_D and the Hill coefficient h were calculated for myosin binding in the presence of c-MyBPC by fitting the data to the Hill equation. (C) K_{obs} plotted as a function of myosin concentration for myosin (■) and 7:1 (▼), 3:1 (▲), and 1:1 (●) myosin_c-MyBPC complexes. The second-order rate constants were determined by a linear fit of the data. (D) Binding of porcine c-MyBPC to actin in the absence of myosin. The K_{obs} values were plotted as a function of c-MyBPC concentration, and the second-order rate constants were determined by a linear fit of the data as described above.

transients observed at 25 $^{\circ}\text{C}$ when 1 and 27.5 μM myosin_c-MyBPC complex is mixed with 1 μM pyr.actin in the stopped-flow fluorimeter. The observed transients can be described well by a single-exponential equation with a K_{obs} of 0.38 s^{-1} for 1 μM myosin_c-MyBPC complex and 14.7 s^{-1} for 27.5 μM . K_{obs} values showed a linear dependence on increasing myosin concentration as shown in Figure 2B; however, in the presence

of unphosphorylated c-MyBPC, there is clearly a shift to a sigmoidal dependence, which suggests a regulatory and cooperativity effect of c-MyBPC on binding of myosin to actin. Figure 2B also shows the effect of increasing the ratio of c-MyBPC in the myosin_c-MyBPC complex. When c-MyBPC and myosin are present in a complex in a 1:7 or 1:3 c-MyBPC:myosin ratio, the lag phase is shorter than when c-MyBPC and myosin are present in a complex in a 1:1 ratio. This suggests that the regulatory effect is dependent on c-MyBPC concentration. Figure 2C shows the effect of adding PKA-treated c-MyBPC to the complex. K_{obs} values show a linear dependence on increasing myosin_c-MyBPC.PKA concentration for all three complex ratios in a manner similar to that of the binding of myosin alone, thus suggesting that phosphorylation of c-MyBPC abolishes the regulatory effect. The second-order rate constants for binding of myosin to actin alone and binding of myosin_c-MyBPC.PKA to actin (K_1k_{+2}) are listed in Table 1 and were estimated from a linear fit to the K_{obs} versus myosin or myosin_c-MyBPC plot to be $0.35 \pm 0.02 \text{ M}^{-1} \text{ s}^{-1}$ for myosin alone or 0.32 ± 0.02 , 0.33 ± 0.01 , and $0.33 \pm 0.03 \text{ M}^{-1} \text{ s}^{-1}$ for myosin_c-MyBPC.PKA in 1:1, 3:1, and 7:1 myosin:c-MyBPC ratios, respectively. The K_{obs} of binding of myosin_c-MyBPC to actin with unphosphorylated c-MyBPC exhibited a sigmoidal dependence on protein concentration rather than a linear one; therefore, binding departs from Scheme 1, and a second-order rate constant (K_1k_{+2}) could not be calculated from the plot. The fraction of myosin_c-MyBPC bound to actin (K_D) is also presented in Table 1 and was calculated via the Hill equation to be $6.79 \pm 0.09 \mu\text{M}$ with a cooperativity h of 5.89 ± 0.22 for a 7:1 myosin:c-MyBPC ratio, $11.48 \pm 0.75 \mu\text{M}$ with an h of 3.54 ± 0.67 for a 3:1 myosin:c-MyBPC ratio, and $16.44 \pm 0.33 \mu\text{M}$ with an h of 9.24 ± 1.34 for a 1:1 myosin:c-MyBPC ratio. Binding of c-MyBPC to actin alone (Figure 2D) shows a modest linear increase in the K_{obs} values with an increase in c-MyBPC concentration, and a much slower second-order rate constant compared to that of binding of myosin and actin alone (Table 1). Thus, c-MyBPC directly binds to actin, but its relative contribution to the measured actin binding signal in the presence of myosin is significantly smaller than that of myosin.

ATP-Induced Actomyosin_c-MyBPC Dissociation. The ATP-induced dissociation of the actomyosin complex can be followed by monitoring the increase in the fluorescence of pyr.actin after the addition of ATP. Figure 3A shows representative fluorescence transients observed at 25 $^{\circ}\text{C}$ when 2 μM actomyosin_c-MyBPC is mixed with 50 and 500 μM ATP in the stopped-flow fluorimeter. The observed transient for myosin_c-MyBPC was described well by a single-exponential equation at both 50 and 500 μM ATP with observed rate constants (K_{obs}) of 22 s^{-1} at 50 μM ATP and 190 s^{-1} at 500 μM ATP. The second-order rate constants for ATP-induced dissociation of actomyosin, actomyosin_c-MyBPC, and actomyosin_c-MyBPC.PKA (K_1k_{+2}) as described in Scheme 2 are listed in Table 1 and were estimated from the linear fit to the plot of K_{obs} versus ATP concentration.

The second-order rate constant for ATP-induced dissociation from actin in the absence of c-MyBPC (K_1k_{+2}) was measured to be $0.42 \pm 0.01 \text{ M}^{-1} \text{ s}^{-1}$. In the presence of unphosphorylated c-MyBPC where myosin and c-MyBPC are in a 1:1 ratio, the rate of dissociation decreases ~3.5-fold compared to that for myosin alone with a second-order rate constant of $0.12 \pm 0.01 \text{ M}^{-1} \text{ s}^{-1}$, suggesting that the presence of c-MyBPC slows the dissociation of myosin from actin in the presence of ATP. This regulatory

Table 1. Calculated Data for the Binding of Myosin to Actin and the ATP-Induced Dissociation of Actomyosin in the Absence and Presence of c-MyBPC^a

	binding to actin			ATP-induced dissociation
	K_1k_{+2} ($M^{-1} s^{-1}$)	K_D (μM)	h	K_1k_{+2} ($M^{-1} s^{-1}$)
myosin	0.35 ± 0.02	ND	ND	0.42 ± 0.01
7:1 myosin_MyBPC	ND	6.79 ± 0.09	5.89 ± 0.22	0.39 ± 0.01
3:1 myosin_MyBPC	ND	11.48 ± 0.75	3.54 ± 0.67	0.22 ± 0.01^b
1:1 myosin_MyBPC	ND	16.44 ± 0.33	9.24 ± 1.34	0.12 ± 0.02^b
7:1 myosin_MyBPC.PKA	0.33 ± 0.03	ND	ND	0.41 ± 0.01
3:1 myosin_MyBPC.PKA	0.33 ± 0.01	ND	ND	$0.29 \pm 0.01^{b,c}$
1:1 myosin_MyBPC.PKA	0.32 ± 0.02	ND	ND	$0.23 \pm 0.01^{b,c}$
MyBPC	0.0004 ± 0.02^b	ND	ND	—

^aData are means \pm the standard deviation, from at least three separate measurements. K_1k_{+2} is the observed value of the second-order rate constant for ATP-induced dissociation of actomyosin in the presence and absence of c-MyBPC and for binding of myosin to actin in the absence of c-MyBPC and in the presence of phosphorylated c-MyBPC and was measured from the plots in Figures 2 and 3. K_1k_{+2} for binding to actin in the presence of myosin could not be measured for unphosphorylated c-MyBPC. K_D values and the Hill coefficient (h) for the binding of myosin to actin in the presence of unphosphorylated c-MyBPC were measured from the best fit to the Hill equation from the plots in Figure 2 (these variables were not observed with phosphorylated c-MyBPC). K_D is measured as the concentration of myosin_c-MyBPC at which the actin filament is half-saturated. ND means not detected. ^bSignificantly different compared to the value for myosin alone. ^cSignificantly different compared to the value for the non-PKA-treated sample.

effect of c-MyBPC does not appear to be cooperative unlike the case for the binding of myosin to actin. In the presence of unphosphorylated c-MyBPC where myosin and c-MyBPC are in a 7:1 ratio, the rate of dissociation is similar to that for myosin alone with a second-order rate constant of $0.39 \pm 0.02 M^{-1} s^{-1}$; however, at a 3:1 ratio, the rate of dissociation is reduced ~ 2 -fold relative to that for myosin alone with a second-order rate constant of $0.22 \pm 0.01 M^{-1} s^{-1}$. The ATP-induced dissociation of actin from myosin in the presence of phosphorylated c-MyBPC where myosin and c-MyBPC are in a 1:1 ratio also decreases ~ 1.5 -fold relative to that for actomyosin alone with a second-order rate constant of $0.23 \pm 0.01 M^{-1} s^{-1}$, but it is increased ~ 2 -fold compared with that for ATP-induced actomyosin dissociation in the presence of unphosphorylated c-MyBPC. This regulatory effect also does not appear to be cooperative, and the phosphorylation of c-MyBPC appears to partially weaken the effects of c-MyBPC regulation on ATP-induced dissociation of actin from myosin. The rate of ATP-induced dissociation of actin from myosin in the presence of phosphorylated c-MyBPC where myosin and c-MyBPC are in a 7:1 ratio did not significantly deviate from the rate of dissociation of myosin from actin alone; however, at a 3:1 ratio, the rate of ATP-induced dissociation of actin from myosin decreases ~ 1.5 -fold compared to that for myosin alone with a second-order rate constant of $0.29 \pm 0.01 M^{-1} s^{-1}$ and is significantly increased ~ 0.5 -fold compared to the rate of unphosphorylated c-MyBPC at a 3:1 ratio with myosin (Table 1).

ATPase Activity. The steady-state ATPase activity of myosin in the absence and presence of c-MyBPC and c-MyBPC.PKA where myosin and c-MyBPC are at a 1:1 or 3:1 myosin:c-MyBPC ratio was measured using the NADH-coupled assay.^{47,48} The release of P_i and ADP from the myosin motor can be conveniently followed by the change in absorbance of NADH at 340 nm after the addition of ATP. The change in absorbance over time in all cases was linear with a negative slope, and from these data, a plot of ADP production versus time was generated. The slope of this plot yielded the steady-state ATPase rate, and this was normalized by plotting the steady-state ATPase rate versus myosin_c-MyBPC concentration. Plots of the steady-state ATPase rate versus

myosin and myosin_c-MyBPC concentration are shown in Figure 4. The steady-state ATPase rate of myosin alone is described as a linear function of its concentration as $0.015 \pm 0.002 s^{-1}$. The steady-state rate of ATPase with myosin_c-MyBPC at a 1:1 or 3:1 myosin:c-MyBPC ratio is described as a sigmoidal function of its concentration, and the rate could not be accurately measured; however, the presence of c-MyBPC appears to significantly slow ATPase rates at low myosin concentrations (Figure 4). K_{cat} is the maximal activated ATPase rate of myosin_c-MyBPC, and K_{ATPase} is the concentration of myosin_c-MyBPC needed to reach half-maximal activation of myosin ATPase activity. The values of these two quantities are $0.24 \pm 0.01 s^{-1}$ and $8.66 \pm 0.15 \mu M$ for myosin and c-MyBPC in a 1:1 ratio and $0.23 \pm 0.02 s^{-1}$ and $5.96 \pm 0.20 \mu M$ for myosin and c-MyBPC in a 3:1 ratio, respectively.

The steady-state ATPase rate of myosin in the presence of phosphorylated c-MyBPC at 1:1 and 3:1 ratios with myosin was also determined. The ATPase rate for myosin in the presence of phosphorylated c-MyBPC at 1:1 and 3:1 ratios with myosin was described as a linear function of myosin_c-MyBPC.PKA concentration and was calculated to be 0.006 ± 0.001 and $0.005 \pm 0.001 s^{-1}$, respectively. The rates in the presence of phosphorylated c-MyBPC were reduced compared to the rate for myosin alone; however, at least in the case of myosin_c-MyBPC at a 1:1 ratio, c-MyBPC phosphorylation appeared to relieve the inhibitory effect of c-MyBPC on ATPase rates at low myosin concentrations (Figure 4).

DISCUSSION

The purpose of this study was to elucidate the functional effects of c-MyBPC on the kinetics of key steps in the cross-bridge cycle of cardiac muscle contraction. Previous studies using skinned cardiac fibers or in vitro motility assays have demonstrated a regulatory role for c-MyBPC in cardiac muscle contraction;^{5,7,11–18} however, the role of c-MyBPC in the regulation of specific steps within the cross-bridge cycle has yet to be clearly established. In this study, we demonstrate that c-MyBPC regulates at least two key steps in the cross-bridge cycle that modulate cross-bridge association and dissociation from actin, and that some of the effects of c-MyBPC are mediated by affecting the cooperative behavior of cross-bridges,

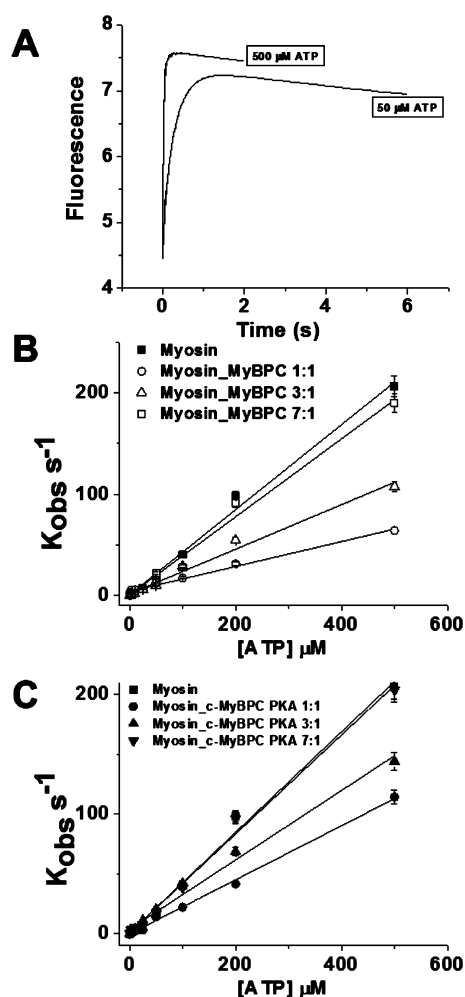


Figure 3. ATP-induced dissociation of myosin from actin in the presence of c-MyBPC. (A) Representative transients for the ATP-induced dissociation of a 2 μ M pyrene-labeled actomyosin_c-MyBPC complex mixed with 50 and 500 μ M ATP. The observed transient of the pyr.actomyosin_c-MyBPC complex was fit to a single-exponential equation, and the observed rate constant K_{obs} was calculated for each ATP concentration. Conditions: 20 mM MOPS, (pH 7.0), 500 mM KCl, and 5 mM $MgCl_2$. (B) K_{obs} plotted as a function of ATP concentration (range of 2.5–500 μ M) for myosin (■) and 1:1 (○), 3:1 (△), and 7:1 (□) myosin_c-MyBPC complexes. The second-order rate constants for the reactions (K_1k_{+2}) were determined by the linear fit of the data. (C) K_{obs} plotted as a function of ATP concentration (range of 2.5–500 μ M) for myosin (■) and 1:1 (●), 3:1 (▲), and 7:1 (▼) myosin_c-MyBPC.PKA complexes. The second-order rate constants for the reactions (K_1k_{+2}) were determined by the linear fit of the data.

even in the absence of thin filament regulation. Finally, we show that PKA-induced phosphorylation of c-MyBPC regulates rates of actomyosin interactions, thereby providing the heart with a molecular mechanism that modulates the rates of cross-bridge cycling to match circulatory demands.

Effects of c-MyBPC on the Kinetics of Binding of Myosin to Actin. The kinetic pathway that describes the binding of myosin to actin is described in Scheme 1, and as expected, binding of myosin to actin in the absence of c-MyBPC exhibited K_{obs} values that were dependent upon myosin concentration, and the second-order rate constants could be easily determined from the gradient of the plot of K_{obs} versus myosin concentration (Figure 2). Our data show that

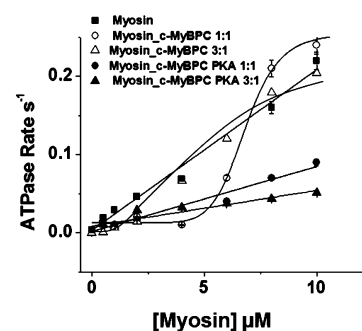


Figure 4. Steady-state ATPase activity of myosin in the presence of c-MyBPC. The activation of ATPase activity is shown as a function of myosin concentration (■) and in the presence of a 1:1 myosin_c-MyBPC (○), a 1:1 myosin_c-MyBPC.PKA complex (●), a 3:1 myosin_c-MyBPC complex (△), and a 3:1 myosin_c-MyBPC.PKA complex (▲) using the NADH-coupled system. The actin concentration was 3.5 μ M, and myosin concentrations ranged from 0.5 to 10 μ M. Conditions: 20 mM MOPS, 500 mM KCl, and 5 mM $MgCl_2$.

unphosphorylated c-MyBPC regulates the binding of myosin to actin and that the mechanism of regulation does not adhere to the kinetic pathway represented in Scheme 1. The mechanism of regulation is cooperative as indicated by the sigmoidal relationship of K_{obs} when both unphosphorylated c-MyBPC and myosin are present, compared to the linear relationship of K_{obs} when only myosin is present (Figure 2). This cooperative binding by the porcine myosin as a consequence of the presence of unphosphorylated c-MyBPC was exhibited also when in the presence of a recombinant mouse full-length c-MyBPC (data not shown), suggesting that these effects are not species specific but rather a characteristic of c-MyBPC. At low myosin concentrations, the presence of c-MyBPC appears to inhibit the binding of myosin to actin as a lag is observed in the increase in the rate of binding of myosin to actin (Figure 2B), consistent with an inhibitory effect of c-MyBPC on myosin binding. This inhibition also appears to be dependent on c-MyBPC concentration, as at a 7:1 myosin:c-MyBPC ratio, the lag is smaller and the inhibition is more easily overcome at relatively low myosin concentrations. However, at 1:3 and 1:1 c-MyBPC:myosin ratios, the lag becomes progressively longer and a much higher myosin concentration is needed to overcome the inhibition of c-MyBPC on myosin binding to actin. Because the physiological ratio of myosin to c-MyBPC in the sarcomere is thought to be as high as 3:1 in the C-zone,^{20,49} it is reasonable to suggest that c-MyBPC would impart significant inhibition to the binding of myosin to actin in vivo. At higher myosin concentrations, there appears to be c-MyBPC-induced activation, whereby binding of myosin to actin is accelerated when compared with binding of myosin to actin alone (Figure 2B).

Previous studies suggested that c-MyBPC binds actin via its N-terminal^{6,8,18,20–27,50,51} or C-terminal⁵² domains; however, the stage of the cross-bridge cycle at which c-MyBPC interacts with actin has not been established. The cooperativity observed when myosin binds actin in the presence of c-MyBPC even at a 1:7 c-MyBPC:myosin ratio may suggest that c-MyBPC can bind actin together with myosin. Our data do not distinguish whether c-MyBPC is detached from myosin when myosin binds actin, or when the c-MyBPC domain binds to actin. We observed, however, that c-MyBPC does bind actin alone (Figure 2D), but the rate is slower compared to the rate of

binding of myosin to actin; thus, it is unlikely that direct binding of c-MyBPC to actin significantly contributes to the observed acceleration of actomyosin association with an increasing myosin concentration. The observed lag phase in the binding of myosin to actin, which is dependent on c-MyBPC concentration, can be explained by a mechanism in which c-MyBPC inhibits binding of myosin to actin, perhaps by tethering the S2 region of myosin.^{14,15} Alternatively, it may be due to direct competition by c-MyBPC and myosin for actin binding sites, such that at low myosin concentrations c-MyBPC is able to bind actin more efficiently. Although binding of c-MyBPC to actin had only modest effects on K_{obs} , this binding could be significant in vivo as recent structural studies have suggested that the N-terminal domains of c-MyBPC bind actin in the same region as Tm at low Ca^{2+} concentrations, which may lead to the destabilization of tropomyosin from the blocked position, thereby favoring thin filament activation.^{6,24,27} Therefore, even weak binding of c-MyBPC to actin could significantly activate the thin filament to accelerate rates of force development.

The activation of binding of myosin to actin in the presence of c-MyBPC at higher myosin concentrations suggests that c-MyBPC facilitates a degree of synergy between adjacent S1 heads and adjacent myosin molecules that enhances cooperative binding to actin, such that initial binding of S1 heads recruits binding of additional S1 heads. In the absence of c-MyBPC, myosin will bind actin with a 1:1 stoichiometry, resulting in a linear relationship (Figure 2B); however, the presence of unphosphorylated c-MyBPC gives rise to more efficient S1 binding, which increases the number of S1 heads that interact with actin, perhaps because of changes in S1 alignment and/or stabilization of S1 heads that favors actin binding. Alternatively, c-MyBPC may give rise to a reordering of the S1 heads at low myosin concentrations toward actin binding sites,^{6,27} thereby accelerating cross-bridge binding and transitions to strongly bound states. Although our data do not support a clear mechanism by which c-MyBPC interacts with adjacent myosins, there is some evidence that the C0 domain and the proline-alanine (PA) domain may play a role in this mechanism as there has been some suggestion that these domains interact with the S1–S2 myosin hinge and the RLC regions of myosin.^{19,53} It is conceivable, therefore, that c-MyBPC could interact with adjacent RLC molecules to better stabilize the S1 heads of more than one myosin molecule. Taken together, these data suggest that c-MyBPC enhances force generation by enhancing cross-bridge binding and cooperative recruitment by direct effects on cross-bridge binding and/or orientation, and indirectly via actin binding, which would enhance thin filament activation.

Effects of c-MyBPC on the ATP-Induced Dissociation of Myosin from Actin. Dissociation of myosin from actin in the absence of c-MyBPC exhibited K_{obs} values that increased with an increasing ATP concentration,^{54–56} and the second-order rate constants as described in Scheme 2 could be easily determined from the gradient of the plot of K_{obs} versus myosin concentration (Figure 3B,C). In the presence of unphosphorylated c-MyBPC, the second-order rate constant for dissociation was decreased ~3.5- and ~2-fold when c-MyBPC was in 1:1 and 1:3 ratios with myosin, respectively, compared with that for myosin alone; however, at a low c-MyBPC concentration (i.e., at a 1:7 ratio with myosin), c-MyBPC had only small effects on dissociation rates (Figure 3B). The reduction in dissociation rates in the presence of c-MyBPC compared to that with

myosin alone suggests that c-MyBPC slows cross-bridge detachment and agrees with in vitro motility data that show that actin filament sliding velocity is reduced in the presence of unphosphorylated c-MyBPC.^{18,20} These studies suggest that c-MyBPC directly interacts with actin at high ATP concentrations because of the lower affinity of myosin S1 for actin under those conditions, and this interaction could lead to the reduction in the rate of dissociation that we observe in our studies. It has been suggested that a population of slowly cycling cross-bridges could give rise to a viscous drag force that limits muscle shortening velocity,⁵⁷ and it is conceivable that slowly cycling cross-bridges could significantly impact cross-bridge behavior in regions of the sarcomere where c-MyBPC is abundant (i.e., present at a 1:3 ratio with myosin). Furthermore, because c-MyBPC may interact with more than one actin molecule,²⁷ even weak interactions between c-MyBPC and actin could have significant effects on muscle contraction in vivo. Our in vitro studies also agree well with previous studies utilizing skinned fiber preparations that showed that biochemical extraction, or the genetic ablation of c-MyBPC, accelerates shortening velocity,^{13,14,58} presumably because of a weakened inhibition of c-MyBPC on cross-bridge detachment.

Although there is strong evidence that supports binding of c-MyBPC to actin, interactions of c-MyBPC with S2 at this stage of the cross-bridge cycle cannot be ruled out, as it would be possible that a direct interaction between c-MyBPC and S2 could delay one or even both of the S1 heads from detaching, thus creating the viscous drag without directly binding to actin. Regardless of the mechanism, our data show, in agreement with others,^{18,20} that c-MyBPC slows cross-bridge detachment rates and therefore acts as a “brake” on the contractile apparatus.

Effects of c-MyBPC on Actomyosin ATPase Rates. The ATPase activity in the absence and presence of c-MyBPC was determined using the NADH-coupled assay to assess the functional effects of c-MyBPC on the overall rate of ATPase turnover. The data show that the ATPase rate of myosin alone was directly proportional to myosin concentration, which was exhibited as a linear curve, consistent with the 1:1 stoichiometry of actomyosin binding (Figure 4). In the presence of c-MyBPC, the curve exhibited a sigmoidal relationship (Figure 4) similar to that observed with the actomyosin association transient kinetic data. The lag phase exhibited by the ATPase curve confirms in the steady state that at high c-MyBPC concentrations (i.e., at a 1:1 or 1:3 c-MyBPC:myosin ratio), c-MyBPC directly inhibits binding of myosin to actin. Slowed ATPase rates at low myosin concentrations and high c-MyBPC concentrations could be due to both slowed cross-bridge association (Figure 2D) and dissociation (Figure 3B). The inhibition of ATPase rates at high c-MyBPC concentrations is overcome only at a certain myosin concentration threshold, which restores myosin binding; however, the maximal ATPase rate in this instance in the absence of c-MyBPC is not significantly different from that for myosin alone. Our results show that the ATPase activity of the myosin motor is inhibited at low myosin concentrations, consistent with previous studies that showed that c-MyBPC inhibits actomyosin ATPase activity^{18,59,60} in the presence of ATP, while in the absence of ATP myosin binding is restored.⁵⁹

Enhanced cross-bridge binding due to c-MyBPC with increasing myosin concentrations and slower cross-bridge detachment rates enhance force generation by augmenting the number of force-generating cross-bridges at a given time

and their duty ratio, which is consistent with the leftward shift in the force–pCa relationship observed in skinned fibers incubated with N-terminal c-MyBPC peptides.^{8,17,18} A slowing of the ATPase rates in the presence of c-MyBPC could be beneficial in vivo via prevention of premature cross-bridge detachment and, thereby, a truncation in the duration of the systolic ejection phase.^{28,58,61}

Functional Effects of c-MyBPC Phosphorylation on Cross-Bridge Kinetics. Some studies in skinned myocardium have shown that phosphorylation of c-MyBPC accelerates cross-bridge kinetics,^{28–30} while other studies show no effect of PKA-induced phosphorylation of c-MyBPC on cross-bridge kinetics.^{32,33} It has been shown that phosphorylation of c-MyBPC increases the proximity of myosin heads to actin, thereby relieving the tethering constraint imposed by c-MyBPC on myosin heads and increasing the probability of actomyosin interaction.⁶² Other studies involving direct binding of c-MyBPC to actin showed that phosphorylation of c-MyBPC reduces the binding affinity of N-terminal domains of c-MyBPC for actin,²⁵ suggesting that c-MyBPC phosphorylation may act to reduce drag on cross-bridge cycling and accelerate cross-bridge detachment. Our studies showed that during cross-bridge association, phosphorylation of c-MyBPC abolishes the lag phase of binding of the cross-bridge to actin, resulting in a linear K_{obs} versus myosin concentration relationship, which is directly proportional to myosin concentration (Figure 2C), consistent with the kinetic mechanism described in Scheme 1. The second-order rate constant is not significantly different from that for myosin binding alone, and this along with the elimination of the lag phase and sigmoidal curve exhibited by the binding of myosin in the presence of unphosphorylated c-MyBPC strongly suggests that phosphorylation of c-MyBPC abolishes the inhibitory effects of c-MyBPC on actomyosin interactions at low myosin concentrations. Phosphorylation of c-MyBPC, therefore, accelerates the attachment step of the cross-bridge cycle relative to binding in the presence of unphosphorylated c-MyBPC, and the second-order rate constant of this step is closely comparable to that observed for myosin alone (Table 1).

With respect to the ATP-induced dissociation of myosin from actin, phosphorylation of c-MyBPC when present at a 1:1 or 1:3 ratio with myosin significantly increased the rate of dissociation relative to the rate of dissociation in the presence of unphosphorylated c-MyBPC (Table 1). In the presence of both dephosphorylated and phosphorylated c-MyBPC, the K_{obs} versus ATP concentration curves were linear, suggesting that the regulation of c-MyBPC on ATP-induced dissociation is not cooperative (Figure 3B,C) and adheres to the kinetic mechanism described in Scheme 2. This result possibly suggests that c-MyBPC could be bound to actin at this stage of the cross-bridge cycle, in accordance with the idea that c-MyBPC binds actin directly and acts as a brake on cross-bridge kinetics,^{6,8,18,20,24,25,27} which is removed when c-MyBPC is phosphorylated. Because K_{obs} values for rates of dissociation of porcine cardiac myosin alone are ~20% faster than the rate of association, we can speculate that PKA-induced acceleration of cross-bridge dissociation results in accelerated ATPase rates and a shortened cross-bridge duty ratio. In contrast, when c-MyBPC is unphosphorylated, the reduction in kinetics due to cooperative activation of cross-bridge association slows the overall rate of ATPase turnover.

In addition to c-MyBPC, there are several targets of β -agonist stimulation in the myocyte that are critical regulators of in vivo

cardiac function. Increased sympathetic drive is known to accelerate Ca^{2+} cycling in the myocyte and enhances the rate and amount of Ca^{2+} that is released and sequestered by the sarcoplasmic reticulum (SR) (reviewed in 63 and 64). Phosphorylation of phospholamban relieves the inhibition on the Serca2a Ca^{2+} -ATPase pump, allowing more entry of Ca^{2+} into the SR, and phosphorylates ryanodine receptors in the SR, allowing greater Ca^{2+} release, thereby enhancing the amplitude of the Ca^{2+} transient and reducing its duration and contributing to accelerated systolic and diastolic function. At the level of the myofilaments, β -adrenergic stimulation principally phosphorylates the thin filament protein troponin I, resulting in altered interactions with troponin C to weaken its Ca^{2+} binding affinity, thereby allowing accelerated rates of force relaxation (reviewed in refs 65 and 66). Data from this study support a model (depicted in Figure 2S of the Supporting Information) in which c-MyBPC appears to have a dual role in regulating cross-bridge kinetics, which directly affects at least two steps of the cross-bridge cycle in a phosphorylation-dependent manner. c-MyBPC inhibits cross-bridge binding at low myosin concentrations, either by binding to myosin directly or by competing with myosin for actin binding sites, and slows cross-bridge dissociation rates to prolong cross-bridge attachment time, with the net result being enhanced force generation that is sustained for a longer duration. Phosphorylation of c-MyBPC relieves the inhibitory delay on cross-bridge binding and speeds cross-bridge dissociation such that the overall rate of cross-bridge cycling is accelerated. Therefore, in conjunction with accelerated Ca^{2+} handling properties, c-MyBPC and troponin I phosphorylations at the myofilament level fine-tune cross-bridge behavior and motor function to match the augmented contractile requirements of the heart under conditions of increased workload.

■ ASSOCIATED CONTENT

§ Supporting Information

Western blot analysis of residue-specific phosphorylation status in porcine c-MyBPC prior to and following PKA treatment and general models of the effects of c-MyBPC on actomyosin kinetics. This material is available free of charge via the Internet at <http://pubs.acs.org>.

■ AUTHOR INFORMATION

Corresponding Author

*Department of Physiology and Biophysics, School of Medicine, Case Western Reserve University, Cleveland, OH 44106. Telephone: (216) 368-8636. Fax: (216) 368-5586. E-mail: jes199@case.edu.

Funding

This work was funded by American Heart Association Grant 09SDG2050195.

Notes

The authors declare no competing financial interest.

■ ACKNOWLEDGMENTS

We thank Michael Harris for support with the collection and analysis of all stopped-flow data and Rajesh Ramachandran for the collection and analysis of all ATPase data.

■ ABBREVIATIONS

c-MyBPC, cardiac myosin binding protein C; PKA, cAMP-dependent protein kinase A; Tm, tropomyosin; LMM, light

meromyosin domain; HCM, hypertrophic cardiomyopathy; RLC, myosin regulatory light chain; pyr. actin, N-(1-pyrenemethyl)iodoacetamide-labeled actin.

REFERENCES

- (1) Okagaki, T., Weber, F. E., Fischman, D. A., Vaughan, K. T., Mikawa, T., and Reinach, F. C. (1993) The major myosin-binding domain of skeletal muscle MyBP-C (C protein) resides in the COOH-terminal, immunoglobulin C2 motif. *J. Cell Biol.* 123, 619–626.
- (2) Freiburg, A., and Gautel, M. (1996) A molecular map of the interactions between titin and myosin-binding protein C. Implications for sarcomeric assembly in familial hypertrophic cardiomyopathy. *Eur. J. Biochem.* 15, 317–323.
- (3) Moos, C., Mason, C. M., Besterman, J. M., Feng, I. N., and Dubin, J. H. (1978) The binding of skeletal muscle C-protein to F-actin, and its relation to the interaction of actin with myosin subfragment-1. *J. Mol. Biol.* 124, 571–586.
- (4) Squire, J. M., Luther, P. K., and Knupp, C. (2003) Structural evidence for the interaction of C-protein (MyBP-C) with actin and sequence identification of a possible actin-binding domain. *J. Mol. Biol.* 331, 713–724.
- (5) Hartzell, H. C., and Titus, L. (1982) Effects of cholinergic and adrenergic agonists on phosphorylation of a 165,000-dalton myofibrillar protein in intact cardiac muscle. *J. Biol. Chem.* 257, 2111–2120.
- (6) Mun, J. Y., Gulick, J., Robbins, J., Woodhead, J., Lehman, W., and Craig, R. (2011) Electron microscopy and 3D reconstruction of F-actin decorated with cardiac myosin-binding protein C (cMyBP-C). *J. Mol. Biol.* 410, 214–225.
- (7) Hofmann, P. A., Hartzell, H. C., and Moss, R. L. (1991) Alterations in Ca^{2+} sensitive tension due to partial extraction of C-protein from rat skinned cardiac myocytes and rabbit skeletal muscle fibers. *J. Gen. Physiol.* 97, 1141–1163.
- (8) Razumova, M. V., Bezold, K. L., Tu, A. Y., Regnier, M., and Harris, S. P. (2008) Contribution of the myosin binding protein C motif to functional effects in permeabilized rat trabeculae. *J. Gen. Physiol.* 132, 575–585.
- (9) Oakley, C. E., Hambly, B. D., Curmi, P. M., and Brown, L. J. (2004) Myosin binding protein C: Structural abnormalities in familial hypertrophic cardiomyopathy. *Cell Res.* 14, 95–110.
- (10) Harris, S. P., Bartley, C. R., Hacker, T. A., McDonald, K. S., Douglas, P. S., Greaser, M. L., Powers, P. A., and Moss, R. L. (2002) Hypertrophic cardiomyopathy in cardiac myosin binding protein-C knockout mice. *Circ. Res.* 90, 594–601.
- (11) Stelzer, J. E., Dunning, S. B., and Moss, R. L. (2006) Ablation of cardiac myosin-binding protein-C accelerates stretch activation in murine skinned myocardium. *Circ. Res.* 98, 1212–1218.
- (12) Stelzer, J. E., Fitzsimons, D. P., and Moss, R. L. (2006) Ablation of myosin-binding protein-C accelerates force development in mouse myocardium. *Biophys. J.* 90, 4119–4127.
- (13) Korte, F. S., McDonald, K. S., Harris, S. P., and Moss, R. L. (2003) Loaded shortening, power output, and rate of force redevelopment are increased with knockout of cardiac myosin binding protein-C. *Circ. Res.* 93, 752–758.
- (14) Hofmann, P. A., Greaser, M. L., and Moss, R. L. (1991) C-protein limits shortening velocity of rabbit skeletal muscle fibres at low levels of Ca^{2+} activation. *J. Physiol.* 439, 701–715.
- (15) Calaghan, S. C., Trinick, J., Knight, P. J., and White, E. (2000) A role for C-protein in the regulation of contraction and intracellular Ca^{2+} in intact rat ventricular myocytes. *J. Physiol.* 528, 151–156.
- (16) Kunst, G., Kress, K. R., Gruen, M., Uttenweiler, D., Gautel, M., and Fink, R. H. (2000) Myosin binding protein C, a phosphorylation-dependent force regulator in muscle that controls the attachment of myosin heads by its interaction with myosin S2. *Circ. Res.* 86, 51–58.
- (17) Harris, S. P., Rostkova, E., Gautel, M., and Moss, R. L. (2004) Binding of myosin binding protein-C to myosin subfragment S2 affects contractility independent of a tether mechanism. *Circ. Res.* 95, 930–936.

- (18) Razumova, M. V., Shaffer, J. F., Tu, A. Y., Flint, G. V., Regnier, M., and Harris, S. P. (2006) Effects of the N-terminal domains of myosin binding protein-C in an in vitro motility assay: Evidence for long-lived cross-bridges. *J. Biol. Chem.* 281, 35846–35854.
- (19) Ababou, A., Rostkova, E., Mistry, S., Le Masurier, C., Gautel, M., and Pfuhl, M. (2008) Myosin binding protein C positioned to play a key role in regulation of muscle contraction: Structure and interactions of domain C1. *J. Mol. Biol.* 384, 615–630.
- (20) Saber, W., Begin, K. J., Warshaw, D. M., and VanBuren, P. (2008) Cardiac myosin binding protein-C modulates actomyosin binding and kinetics in the in vitro motility assay. *J. Mol. Cell. Cardiol.* 44, 1053–1061.
- (21) Kulikovskaya, I., McClellan, G., Flavigny, J., Carrier, L., and Winegrad, S. (2003) Effect of MyBP-C binding to actin on contractility in heart muscle. *J. Gen. Physiol.* 122, 761–774.
- (22) Jeffries, C. M., Whitten, A. E., Harris, S. P., and Trewella, J. (2008) Human cardiac myosin binding protein C: Structural flexibility within an extended modular architecture. *J. Mol. Biol.* 377, 1186–1199.
- (23) Whitten, A. E., Jeffries, C. M., Harris, S. P., and Trewella, J. (2008) Cardiac myosin-binding protein C decorates F-actin: Implications for cardiac function. *Proc. Natl. Acad. Sci. U.S.A.* 105, 18360–18365.
- (24) Orlova, A., Galkin, V. E., Jeffries, C. M., Egelman, E. H., and Trewella, J. (2011) The N-terminal domains of myosin binding protein C can bind polymorphically to F-actin. *J. Mol. Biol.* 412, 379–386.
- (25) Shaffer, J. F., Kensler, R. W., and Harris, S. P. (2009) The myosin-binding protein C motif binds to F-actin in a phosphorylation-sensitive manner. *J. Biol. Chem.* 284, 12318–12327.
- (26) Kensler, R. W., Shaffer, J. F., and Harris, S. P. (2011) Binding of the N-terminal fragment C0–C2 of cardiac MyBP-C to cardiac F-actin. *J. Struct. Biol.* 174, 44–51.
- (27) Luther, P. K., Winkler, H., Taylor, K., Zoghbi, M. E., Craig, R., Padrón, R., Squire, J. M., and Liu, J. (2011) Direct visualization of myosin-binding protein C bridging myosin and actin filaments in intact muscle. *Proc. Natl. Acad. Sci. U.S.A.* 108, 11423–11428.
- (28) Stelzer, J. E., Patel, J. R., Walker, J. W., and Moss, R. L. (2007) Differential roles of cardiac myosin-binding protein C and cardiac troponin I in the myofibrillar force responses to protein kinase A phosphorylation. *Circ. Res.* 101, 503–511.
- (29) Tong, C. W., Stelzer, J. E., Greaser, M. L., Powers, P. A., and Moss, R. L. (2008) Acceleration of cross-bridge kinetics by protein kinase A phosphorylation of cardiac myosin binding protein C modulates cardiac function. *Circ. Res.* 103, 974–982.
- (30) Chen, P. P., Patel, J. R., Rybakova, I. N., Walker, J. W., and Moss, R. L. (2010) Protein kinase A-induced myofilament desensitization to Ca^{2+} as a result of phosphorylation of cardiac myosin-binding protein C. *J. Gen. Physiol.* 136, 615–627.
- (31) Barefield, D., and Sadayappan, S. (2010) Phosphorylation and function of cardiac myosin binding protein-C in health and disease. *J. Mol. Cell. Cardiol.* 48, 866–875.
- (32) Verduyn, S. C., Zaremba, R., van der Velden, J., and Stienen, G. J. (2007) Effects of contractile protein phosphorylation on force development in permeabilized rat cardiac myocytes. *Basic Res. Cardiol.* 102, 476–487.
- (33) Walker, J. S., Walker, L. A., Margulies, K., Buttrick, P., and de Tombe, P. (2011) Protein kinase A changes calcium sensitivity but not cross-bridge kinetics in human cardiac myofibrils. *Am. J. Physiol.* 301, H138–H146.
- (34) Malik, F. I., Hartman, J. J., Elias, K. A., Morgan, B. P., Rodriguez, H., Brejc, K., Anderson, R. L., Sueoka, S. H., Lee, K. H., Finer, J. T., Sakowicz, R., Baliga, R., Cox, D. R., Garard, M., Godinez, G., Kawa, R., Kraynack, E., Lenzi, D., Lu, P. P., Muci, A., Niu, C., Qian, X., Pierce, D. W., Pokrovskii, M., Suehiro, I., Sylvester, S., Tochimoto, T., Valdez, C., Wang, W., Katori, T., Kass, D. A., Shen, Y. T., Vatner, S. F., and Morgans, D. J. (2011) Cardiac myosin activation: A potential therapeutic approach for systolic heart failure. *Science* 18, 1439–1443.

- (35) Szczesna, D., Zhao, J., and Potter, J. D. (1996) The regulatory light chains of myosin modulate cross-bridge cycling in skeletal muscle. *J. Biol. Chem.* 271, 5246–5250.
- (36) Stelzer, J. E., Patel, J. R., and Moss, R. L. (2006) Acceleration of stretch activation in murine myocardium due to phosphorylation of myosin regulatory light chain. *J. Gen. Physiol.* 128, 261–272.
- (37) Geeves, M. A., Goody, R. S., and Gutfreund, H. (1984) Kinetics of acto-S1 interaction as a guide to a model for the cross-bridge cycle. *J. Muscle Res. Cell Motil.* 5, 351–361.
- (38) Smith, D. A., and Geeves, M. A. (1995) Strain-dependent cross-bridge cycle for muscle. *Biophys. J.* 69, 524–537.
- (39) Eisenberg, E., and Kielley, W. W. (1970) Native tropomyosin: Effect on the interaction of actin with heavy meromyosin and subfragment-1. *Biochem. Biophys. Res. Commun.* 40, 50–56.
- (40) Szent-Györgyi, A. G. (1975) Calcium regulation of muscle contraction. *Biophys. J.* 15, 707–723.
- (41) McKillop, D. F., and Geeves, M. A. (1993) Regulation of the interaction between actin and myosin subfragment 1: Evidence for three states of the thin filament. *Biophys. J.* 65, 693–670.
- (42) Vibert, P., Craig, R., and Lehman, W. (1997) Steric model for activation of muscle thin filaments. *J. Mol. Biol.* 266, 8–14.
- (43) Hartzell, H. C., and Sale, W. S. (1985) Structure of C protein purified from cardiac muscle. *J. Cell Biol.* 100, 208–215.
- (44) Starr, R., and Offer, G. (1978) The interaction of C-protein with heavy meromyosin and subfragment-2. *Biochem. J.* 171, 813–816.
- (45) Weeds, A. G., and Taylor, R. S. (1975) Separation of subfragment-1 isoenzymes from rabbit skeletal muscle myosin. *Nature* 257, 54–56.
- (46) Spudich, J. A., and Watt, S. (1971) The regulation of rabbit skeletal muscle contraction. I. Biochemical studies of the interaction of the tropomyosin-troponin complex with actin and the proteolytic fragments of myosin. *J. Biol. Chem.* 246, 4866–4871.
- (47) Furch, M., Geeves, M. A., and Manstein, D. J. (1998) Modulation of actin affinity and actomyosin adenosine triphosphatase by charge changes in the myosin motor domain. *Biochemistry* 37, 6317–6326.
- (48) De La Cruz, E. M., and Ostap, E. M. (2009) Kinetic and equilibrium analysis of the myosin ATPase. *Methods Enzymol.* 455, 157–192.
- (49) Craig, R., and Offer, G. (1976) Axial arrangement of cross-bridges in thick filaments of vertebrate skeletal muscle. *J. Mol. Biol.* 102, 325–332.
- (50) Herron, T. J., Rostkova, E., Kunst, G., Chaturvedi, R., Gautel, M., and Kentish, J. C. (2006) Activation of myocardial contraction by the N-terminal domains of myosin binding protein-C. *Circ. Res.* 98, 1290–1298.
- (51) Weith, A., Sadayappan, S., Gulick, J., Previs, M. J., Vanburen, P., Robbins, J., and Warshaw, D. M. (2012) Unique single molecule binding of cardiac myosin binding protein-C to actin and phosphorylation-dependent inhibition of actomyosin motility requires 17 amino acids of the motif domain. *J. Mol. Cell. Cardiol.* 52, 219–227.
- (52) Rybakova, I. N., Greaser, M. L., and Moss, R. L. (2011) Myosin binding protein C interaction with actin: Characterization and mapping of the binding site. *J. Biol. Chem.* 286, 2008–2016.
- (53) Ratti, J., Rostkova, E., Gautel, M., and Pfuhl, M. (2011) Structure and interactions of myosin-binding protein C domain C0: Cardiac-specific regulation of myosin at its neck? *J. Biol. Chem.* 286, 12650–12658.
- (54) White, H. D., and Taylor, E. W. (1976) Energetics and mechanism of actomyosin adenosine triphosphatase. *Biochemistry* 15, 5818–5826.
- (55) Criddle, A. H., Geeves, M. A., and Jeffries, T. (1985) The use of actin labelled with N-(1-pyrenyl) iodoacetamide to study the interaction of actin with myosin subfragments and troponin/tropomyosin. *Biochem. J.* 232, 343–349.
- (56) Nyitrai, M., Ross, I. R., Adamek, N., Pellegrino, M. A., Bottinelli, R., and Geeves, M. A. (2006) What limits the velocity of fast-skeletal muscle contraction in mammals? *J. Mol. Biol.* 355, 432–442.
- (57) Moss, R. L. (1986) Effects on shortening velocity of rabbit skeletal muscle due to variations in the level of thin-filament activation. *J. Physiol.* 377, 487–505.
- (58) Palmer, B. M., Georgakopoulos, D., Janssen, P. M., Wang, Y., Alpert, N. R., Belardi, D. F., Harris, S. P., Moss, R. L., Burgon, P. G., Seidman, C. E., Seidman, J. G., Maughan, D. W., and Kass, D. A. (2004) Role of cardiac myosin binding protein C in sustaining left ventricular systolic stiffening. *Circ. Res.* 94, 1249–1255.
- (59) Moos, C., Mason, C. M., Besterman, J. M., Feng, I. N., and Dubin, J. H. (1978) The binding of skeletal muscle C-protein to F-actin, and its relation to the interaction of actin with myosin subfragment-1. *J. Mol. Biol.* 124, 571–586.
- (60) Julian, F. J., and Moss, R. L. (1980) Sarcomere length-tension relations of frog skinned muscle fibers at lengths above the optimum. *J. Physiol.* 304, 529–539.
- (61) Nagayama, T., Takimoto, E., Sadayappan, S., Mudd, J. O., Seidman, J. G., Robbins, J., and Kass, D. A. (2007) Control of in vivo left ventricular [correction] contraction/relaxation kinetics by myosin binding protein C: Protein kinase A phosphorylation dependent and independent regulation. *Circulation* 116, 2399–2408.
- (62) Colson, B. A., Bekyarova, T., Locher, M. R., Fitzsimons, D. P., Irving, T. C., and Moss, R. L. (2008) Protein kinase A-mediated phosphorylation of cMyBP-C increases proximity of myosin heads to actin in resting myocardium. *Circ. Res.* 103, 244–251.
- (63) Bers, D. M. (2008) Calcium cycling and signaling in cardiac myocytes. *Annu. Rev. Physiol.* 70, 23–49.
- (64) Grimm, M., and Brown, J. H. (2010) β -Adrenergic receptor signaling in the heart: Role of CaMKII. *J. Mol. Cell. Cardiol.* 48, 322–330.
- (65) Layland, J., Solaro, R. J., and Shah, A. M. (2005) Regulation of cardiac contractile function by troponin I phosphorylation. *Cardiovasc. Res.* 66, 12–21.
- (66) Solaro, R. J. (2008) Multiplex kinase signaling modifies cardiac function at the level of sarcomeric proteins. *J. Biol. Chem.* 283, 26829–26833.